An Efficient Energy Recovery Approach of a BLDC Driven E-Rickshaw In Regenerating Braking Mode

Arpita Basu[a*], Madhu Singh[b]

[a*]*Research Scholar, Department of Electrical Engineering, National Institute of Technology, Jamshedpur, Jharkhand-831014, India, +91-9874330014, 2020rsee004@nitjsr.ac.in*

[b]*Associate Professor, Department of Electrical Engineering, National Institute of Technology, Jamshedpur, Jharkhand-831014 India, +91-9431724528, madhu.ee@nitjsr.ac.in*

Abstract

This paper presents the energy recovery efficiency of a Brushless Direct Current (BLDC) motor drive. The primary application of this system is to power an energy-efficient e-rickshaw during regenerative operation. Notably, this work eliminates the need for an additional converter to manage reverse power flow, a crucial step towards realizing a sustainable green transport model. A novel two-boost method is implemented to three phase Voltage Source Inverter (VSI) for bidirectional energy flow connected between battery and the BLDC motor. This approach not only facilitates the transfer of energy from the BLDC motor to the battery but also serves as an effective means of generating braking force. By comparing the proposed two-boost method with the conventional single boost method, it demonstrates that the energy regenerated is significantly higher in this novel approach. To validate the findings, a real time testing on OPAL-RT LAB experimental set up has been used, which validate the results obtained through MATLAB/SIMULINK simulations. This paper contributes to the advancement of energy-efficient transportation solutions, aligning with the growing emphasis on sustainable and environmentally friendly modes of travel.

Keywords: PV array; Regenerative Braking; BLDC Motor; Sensorless Control; Battery Storage

1. Introduction

In the IC engine, carbon dioxide is released by diesel and gasoline, a greenhouse gas which is driving the environment to dangerous levels. Burning fossil fuels like gasoline which is emitted into the atmosphere also caused pollution in the atmosphere. The burden of carbon dioxide (CO_2) and other greenhouse gases like methane (CH_4), nitrous oxide (N_2O), and hydrofluorocarbons (HFCs) in the atmosphere increases the earth's temperature. Consequently, in the human race, climate changes are the biggest challenge. Thomas Davenport was invented a tricycle as a first Electric Vehicle (EV) in 1834. Many authors investigated battery-ultracapacitor storage system in electric vehicle [1]. The main challenges of EV are the short range due to its limited battery capacity. Different intelligent control techniques are used to increase the range of the electric vehicles [2-4]. The proposed intelligent techniques like fuzzy, PSO, ANN, combination of fuzzy and PSO found to be costly and complicated in terms of control strategies.

The literature reveals a growing emphasis on regenerative braking in Electric Vehicles (EVs) as evident in recent research efforts [5]. The pivotal role of the Voltage Source Inverter (VSI) in sustaining energy regeneration is underscored [6, 7]. To optimize regenerative braking, various control techniques are explored [8]. The focus of regenerative braking lies in recuperating otherwise wasted energy during vehicle braking maneuvers. This is especially significant for Light Electric Vehicles (LEVs), such as three-wheeler goods carriers or E-rickshaws, predominantly powered by Brushless DC (BLDC) motors. BLDC motors offer the dual advantage of energy regeneration capability and ease of control. The incorporation of regenerative braking involves the use of an additional DC-DC converter, which elevates the back electromotive force (back-EMF) to the requisite level for efficient battery charging. Studies indicate that in city drive cycles, the energy regeneration potential typically falls within

the range of 8-15% [9, 10]. This work delves into the controlled switching patterns of the VSI, ensuring that the regenerative braking process is executed in an optimal and efficient manner [11-13]. By addressing the intricacies of VSI control strategies, the research aims to contribute to the broader understanding and advancement of regenerative braking systems in EVs, particularly in the context of light electric vehicles.

The proposed system represents a groundbreaking fusion of lithium-ion battery technology and solar energy, ushering in extended driving ranges and substantial reductions in maintenance costs. This hybrid power configuration ensures the system's resilience even in the face of dynamic weather conditions. The integration of a solar panel, working in tandem with a sophisticated battery storage system, augments operational stability. Significantly, during no-load conditions, the lithium-ion battery undergoes charging, taking full advantage of optimal solar insolation. To maximize the utilization of solar energy, a boost converter is strategically employed for Maximum Power Point Tracking (MPPT), a technique well-established in prior research [14]. The Perturb and Observe (P&O) method, a widely endorsed MPPT strategy capable of adapting to variations in irradiation and temperature, is implemented in this scenario. The study also elucidates how the MPPT output is further refined through the integration of a buck converter [15]. Existing literature extensively reviews diverse MPPT methods for photovoltaic (PV) arrays, encompassing models and connection schemes [16, 17]. The selected P&O method distinguishes itself with its inherent advantages, requiring no periodic tuning and offering a user-friendly implementation [18].

In this work, particular emphasis is placed on an innovative regenerative braking approach. This unique strategy leverages the combined power of solar PV and the lithium-ion battery in e-rickshaws. This not only harnesses renewable energy for propulsion but also introduces an efficient means of energy recovery during braking, significantly elevating the overall sustainability and efficiency of the e-rickshaw system.

2. System Configuration

The schematic diagram in Figure 1 represents the overall system. This system comprises of a 300 W Photovoltaic (PV) system, two numbers of converter circuits; battery storage, and a 1kW BLDC motor. PV array, battery systems and BLDC drive are connected to a common DC bus. The boost converter and the PV array is directly connected in series which is used to regulate the MPPT. During charging and discharging of the battery, power flow is regulated by the bi-directional converter. When the power generated by PV array is less than the requisite power for the load, the battery discharges to feed the load to fulfill the end demand. On the other hand, when the power generated by the PV array is greater than the demand, the battery gets charging even when the motor is running idle. 1kW BLDC motor is designed for a 300 W PV array with regenerative braking. A comparative study of various topologies of regenerative braking has been done in this work.

2.1 Sizing of PV panel

Due to the limitation of space availability on the roof of the rickshaw, which is 2.6 +sq. meter the PV array considered is of 300 W peak power. A 300 W PV array is designed by using the model data sheet of Apollo Solar Energy ASEC-300 G65solar panel in MATLAB simulation. In this system for MPPT Perturb & Observation (P&O) method is preferred. Table 1 shows the parameter values of the PV system. The specification of boost converter, buck-boost converter, battery and BLDC motor are shown from Table 2-5.

3. Regenerative braking method

In this section a single boost method and a two-boost method for regenerative braking of BLDC drive have been introduced and discussed in detail. The performance of the two topologies has been studied through MATLAB/SIMULINK simulation and validated using the real time digital simulator.

The circuit representation of BLDC drive is shown in Figure 2. The switching pattern of a BLDC drive in regeneration mode is seen in Figure 3. PWM pulses are used to drive every switch. The EV mode of operation switches instantly from forward driving to regenerating mode when the brake signal is applied, and the switching pattern of the VSI is also altered. The back-emf functions as a voltage source and a VSI as a boost converter during regeneration mode. The boost converter treats the winding inductance as an inductance during regeneration. S_2 and S_3 are turned on in this mode, but in a synchronal PWM manner. Back-emfs in the phase windings of the BLDC motor and Hall-Effect signals are used in the development of the regenerative braking technique and the gating pulses to the VSI.

3.1 Single boost method for regeneration of energy

There are various topologies for three-phase BLDC motor drives have been discussed by many authors [19, 20]. In this system, a three-phase inverter, six power switches and position sensor less control is used to drive the BLDC motor. Figure 2 depicts the circuit presentation of the BLDC drive. The single-boost technique employs a back-emf procedure to produce energy for the BLDC motor drive. The VSI functions like a boost converter while in regenerative mode. The upper half switches are switched off and their body diodes act as a boost converter diode. While the lower half switches are in on-off mode every 60^o of electronic commutation. As shown in Figure 3 the PWM control strategy is used in each stage. After receiving the brake order, the inverter's logical switching gate is modified. As a result, regenerative braking begins.

For the BLDC motor, as the back emf is proportional to the speed of the motor and related to,

$$E = V_K + \omega \qquad (1)$$

Where, V_K and ω are the motor voltage constant and speed respectively. Circuit operation of regenerating mode using single boost method of BLDC drive as shown in Figures 4(a)-(b). Switches S_1, S_3, S_5 are switched off. During (0-π/3), the lower side switches S_2, D_1, and

winding inductance comprises the motor driver's circuit, which is similar to the boost converter as shown in Figure 4(b).

Figure 4(b) depicts the BLDC motor drive equivalent circuit. In this figure, $V_{in} = 2E$, where E represents the motor's back EMF. Calculations utilize a factor of two since the motor operates in two phases simultaneously. $V_0 = v_{bat}$, where $\boldsymbol{v_{bat}}$ is the battery voltage, is the output voltage. The motor's one phase's resistance and inductance are denoted by the letters *R* and *L*, respectively.

The converter can be used to calculate the relationship indicated below if the phrase *2R* is ignored:

$$\frac{v_b}{2E} = \frac{1}{1-d} \qquad (2)$$

Therefore,

$$d = 1 - \frac{2E}{v_b} \qquad (3)$$

Current in motor winding changes, depending on the requirement of the load torque. The negative current flows in the winding, hence on certain operating conditions, inductor current can become discontinuous.

Here, continuous conduction mode (CCM) is taken into consideration. The winding current will be continuous when the motor is operating at high speed and torque. The duty ratio of the boost converter depends on the battery voltage and the back EMF. On the other hand, the back EMF depends on the drive's speed. More energy can be recovered under high-speed condition. The K.E. of the system,

$$K.E. = 0.5\, mv^2 \qquad (4)$$

The energy feedback to the battery during the regenerative process is,

$$E_{waste} = T_L \int_{t_1}^{t_2} \omega(t) dt \qquad (5)$$

Where, m is the mass of the vehicle and t_1 and t_2 are the electrical braking time instant.

Hence, total regenerative braking is,

$$E_{regenration} = K.E. - E_{waste} \qquad (6)$$

Percentage of regenerated power is,

$$\%E_{gen} = \frac{E_{generation}}{K.E.} * 100 \qquad (7)$$

3.2 Two boost method for regeneration of energy

Two boost method is used for the energy regeneration of the BLDC motor shown in Figure 5. VSI acts as a two-boost converter in which each 60^o interval of the electronic commutation. The main drawback of the single boost method is that when the phase of the back-emf changes linearly, it is kept-off. Only the phase with constant back-emf is used for the remaining power flow in the system. However, in the proposed method, three phases get utilized at the same time including the phases whose back-emf is variable. This method increases the amount of regenerated power. The equivalent circuit of the two-boost method is shown in Figure 6. Switches S_4 and S_2 are gated with the duty cycle and S_6 is on in this interval.

Figure 7 shows the switching states of the method. The low side switches i.e., S_2 S_4 S_6 are kept on in the state 1. Whereas, in the state 2 S_4, S_6 are on and only S_6 is on in the state 3. So, for instant at the interval (0-π/3) S_6 is always on with duty cycle 1.

4. Sensorless control technique

A six-step, 120-degree communication technique is used to drive the BLDC motor, with two phases being activated every 60 degrees. Figure 8 illustrates how square wave excitation causes the motor's back emf, which is trapezoidal in shape and leads the phase current and related Hall signal.

The measured line voltages yield three reference voltage signals [21]. The stator resistance R_a, phase inductance L_a, current i_a, and back emf e_{an} in the voltage equation for Phase A are expressed as,

$$V_{an} = R_a\, i_a + L_a \frac{di_a}{dt} + e_{an} \tag{8}$$

For phase B and C,

$$V_{bn} = R_b\, i_b + L_b \frac{di_b}{dt} + e_{bn} \tag{9}$$

$$V_{cn} = R_c\, i_c + L_c \frac{di_c}{dt} + e_{cn} \tag{10}$$

Where the symbols have their usual meanings,

From these equations line voltage V_{ab} can be written as,

$$V_{ab} = V_{an} - V_{bn} = R\,(i_a - i_b) + L\frac{d(i_a - i_b)}{dt} + (e_{an} - e_{bn}) \tag{11}$$

Similarly,

$$V_{bc} = V_{bn} - V_{cn} = R\,(i_b - i_c) + L\frac{d(i_b - i_c)}{dt} + (e_{bn} - e_{cn}) \tag{12}$$

Subtracting (12) from (11),

$$V_{abbc} = R\,(i_b - 2i_b + i_c) + L\frac{d(i_a - 2i_b + i_c)}{dt} + (e_{an} - 2e_{bn} + e_{cn}) \tag{13}$$

During the interval as depicted in Figure 8, phase A and C are conducting, whereas phase B is silent. So, $i_a = -i_c$ and $i_b = 0$. The back emfs of phase A and C are equal and opposite. Substitute these in equation (13) V_{abbc} can be written as,

$$V_{abbc} = V_{ab} - V_{bc} = (e_{an} - 2e_{bn} + e_{cn}) = -2e_{bn} \tag{14}$$

Thus, the derived signal V_{abbc} is nothing but an inverter representation of twice of phase B back emf. V_{bcca} and V_{caab} can likewise be generated similarly. Since the motor's line voltage is independent of speed, the drive can be dynamically controlled using the sensor-less control

technique. The resistance, EMF (RLE representation) and inductance, of the phase (not referring to ground) would contain the EMF values.

5. Control method of sensorless control technique

The starting method of the sensorless control technique is shown in Figure 9. This technique is started by exciting two pre-determined phases. In this case let, phase B and C are taken as a pre-determined phase. By turning on the inverter's PB+ and PC-devices, phase B and phase C of the motor are linked to the positive and negative terminals of the DC power supply, respectively. The pre-positing time (Tp), which is the predetermined duration for which these devices are stimulated, is known.

The rotor changed from an unknown position to a known position at the end of Tp. Phases A and C are then stimulated to produce the motor's maximum torque after that. Phases C and A are excited two switching intervals apart from the initial excitation phases B and C, which are predefined. This allows for a 120-degree rotor rotation, which is sufficient to cause the phase B back-EMF to cross zero at that point. The EMF of phase B then crosses zero once more when phases A and C are activated. Upon detecting the phase B back-EMF's zero-crossing instant, the subsequent commutation (PC+ and PB-) is executed promptly. This guarantees a positive torque development while the rotor rotates in a forward direction. At zero crossing instants, the phase excitation procedure is repeated until the sensorless technique is prepared to commutate to the accurate estimated commutation instants, as indicated in Table 6. Since the phase current and back-EMF directions are made to coincide, the developed torque is always accelerating.

6. Effectiveness of the proposed drive with the commercial drives for BLDC motors

For a variety of reasons, the growing number of electric cars (EVs) is considered an improvement over the current vehicles. This necessitates a thorough examination of the

motor, which forms the basis of these cars. In the propulsion system of an electric vehicle, a motor is an essential component that can have an impact on the power, dependability, weight, cost, and efficiency results and abilities [22]**.** Thus, Table 7 presents the results of a comparative investigation that contrasts the current types with the suggested drive.

7. Protection Schemes

The protection of industrial BLDC drives against overcurrent, electromagnetic compatibility (EMC), and electromagnetic interference (EMI) is essential for reliable and safe operation. The comparative discussion on the required protections in the context of industrial BLDC drives are given in Table 8.

8. Results and Discussion

The whole system is designed by using 300W solar panel and 48V, 80Ah lithium-ion battery feeds 4Nm BLDC motor drive. The system is simulated in MATLAB Environment.

Figure 10 shows the speed and electromagnetic torque of the BLDC motor.

Figure 11 represents the basic performance of the BLDC drive with Stator current, electromotive force, virtual hall signal of phase A in idle condition.

Figure 12 shows the regenerative operation where motor decelerates when speed reduces and battery gets charging. Hence, electromagnetic toque goes to negative as the state-of-charge (SOC) level is increasing.

Figure 13 shows solar panel directly charges the battery even in the absence of the load torque Here, after 1.5 sec, load toque is eliminated and solar insolation level starts rising in the sunny day.

In Table 9 Comparison of two methods is shown. The amount of regenerated power in the single boost method lesser than the proposed method as shown in the table. Moreover, the

simulation results are under closed loop operation, where the proportional-integral-derivate (PID) controller is used to control the speed of the BLDC drive**.**

9. Implementation of RTDS and results

The real time simulator (RTDS) is powerful modulator which is implemented on MATLAB/SIMULINK simulation model. Hardware-in-loop and off-line simulation is used for designing purpose. Figure 14 represents the architecture of RT-LAB. The Hardware setup of the OPAL-RT is shown in Figure 15.

As the naming convention of RT-LAB, there are two subsystems. A prefix identifies the subsystems and also their function. 1. SM_main subsystem which contains the model's computational elements, namely the PV model, boost converter, bidirectional converter, battery and BLDC motor drive (Figure 16). 2. SC_main subsystem includes all user interface blocks. In this system it consists of scope and manual switches as shown in Figure 17.

The PV system's real-time simulation results are shown in Figure 18(a) shows that at t=0-1.5sec, the output power of the PV array is 300 W. At this time interval the solar insolation is 1000W/m^2. At the interval, t=1.5-3sec the insolation decreases and the voltage, current of the PV array decreases respectively as shown in Figure 18(b), (c). Whereas the DC bus voltage maintains a constant voltage of around 48 Volts as shown in Figure 18(d).

The battery is charging when the solar insolation is 1000W/m^2 as shown in Figure 19(a). The battery is discharging and the produced power goes down as a solar insolation is 0W/m^2. As shown in Figure 19(c) there is reverse flow of the battery current (I_{bat}).

Figure 20 shows the real time results of stator current, motor back emf voltage and virtual hall signal of phase A.

10. Conclusion

The presented work introduces an innovative closed-loop two-boost method for driving the BLDC motor. This approach is meticulously compared with the conventional open-loop

single boost method. Through extensive MATLAB/SIMULINK simulations, it is observed that the regenerative braking achieved with the two-boost method surpasses that of the single boost method by an impressive 20%. The simulation results are further scrutinized, and the performance is authenticated through real-time digital simulator experiments. The application of the two-boost method in regenerative braking not only enhances the amount of regenerated energy but also contributes to a notable improvement in the overall system efficiency. The comparative analysis of the two boost methods showcases the superiority of the proposed closed-loop simultaneous boost technique. The real-time validation of the results adds credibility to the findings, reinforcing the effectiveness of employing the simultaneous boost method for regenerative braking in BLDC motor systems. This research thus contributes to advancing the understanding and application of closed-loop control strategies for optimizing the performance of BLDC motors.

References

1. Rezaei, H., Abdollahi, S.E., Abdollahi, S. et al., "Energy management strategies of battery-ultracapacitor hybrid storage systems for electric vehicles: Review, challenges, and future trends", *Journal of Energy Storage*, *53*, pp.105045 (2022). https://doi.org/10.1016/j.est.2022.105045

2. Ramya, A., Balaji, M. and Kamaraj, V. "Adaptive MF tuned fuzzy logic speed controller for BLDC motor drive using ANN and PSO technique", *The Journal of Engineering*, pp. 3947-3950 (2019). https://doi.org/10.1049/joe.2018.8179

3. Gautam, A.K., Tariq, M., Pandey, J.P. et al., "Optimal power management strategy by using fuzzy logic controller for BLDC Motor-Driven E-Rickshaw", *Journal of Intelligent & Fuzzy Systems*, *42*(2), pp. 1089-1098 (2022). https://doi.org/10.3233/JIFS-189774

4. Kumar, S., Roy, D. and Singh, M. "A fuzzy logic controller based brushless DC motor using PFC cuk converter", *International Journal of Power Electronics and Drive Systems*, *10*(4), pp.1894 (2019). https://doi.org/10.11591/ijpeds.v10.i4

5. Sreejith, R. and Singh, B. "Position sensorless PMSM drive for solar PV-battery light electric vehicle with regenerative braking capability", In *2020 IEEE Energy Conversion*

Congress and Exposition (ECCE), pp. 1447-1452 (2020). https://doi.org/10.1109/ECCE44975.2020.9236086

6. Hasanah, R.N., Andrean, V., Suyono, H. et al., "Bidirectional VSI as a regenerative-braking converter for BLDC motor—An analysis on a plug-in electric vehicle application", *10th International Conference on Electrical and Electronics Engineering* (ELECO) pp. 222-226 (2017).

7. Mishra, S., Varshney, A., Singh, B. et al., "Driving Cycle Based Modelling and Control of Solar-Battery fed RelSyn Motor Drive for Light Electric Vehicle with Energy Regeneration", In *2021 IEEE Energy Conversion Congress and Exposition (ECCE)*, pp. 5008-5013 (2021).

8. Deepa, M.U. and Bindu, G.R. "A novel switching scheme for regenerative braking and battery charging for BLDC motor drive used in electric vehicle", *IEEE international power and renewable energy conference* pp. 1-6 (2020).
https://doi.org/10.1109/IPRECON49514.2020.9315226

9. Singh, B. and Saha, B. "Landsman Convereter Based Sensorless BLDC Motor Driven Solar PV-Battery fed E-Rickshaw with Regenerative Braking", *In 2020 IEEE 5th International Conference on Computing Communication and Automation (ICCCA)*, pp. 18-23 (2020). https://doi.org/10.1109/ICCCA49541.2020.9250851

10. Balasubramanian, B. and Huzefa, A.C. "Development of regeneration braking model for electric vehicle range improvement", *IEEE Transportation Electrification Conference* (ITEC-India), pp. 1-5 (2017). https://doi.org/10.1109/ITEC-India.2017.8333825

11. Riyadi, S. and Setianto, Y.D. **"**Analysis and design of BLDC motor control in regenerative braking", International *Symposium on Electrical and Electronics Engineering* (ISEE), pp. 211-215 (2019). https://doi.org/10.1109/ISEE2.2019.8920962

12. Saha, B. and Singh, B. "An Approach for Enhanced Range with Regenerative Braking in Solar PV-Battery Based E-Rickshaw using Sensorless BLDC Motor Drive", In *2020 IEEE International Conference on Computing, Power and Communication Technologies (GUCON)*, pp. 809-814 (2020). https://doi.org/10.1109/GUCON48875.2020.9231254

13. Oliver, J.S., David, P.W., Balachandran, P.K. et al., "Analysis of Grid-Interactive PV-Fed BLDC Pump Using Optimized MPPT in DC–DC Converters", *Sustainability*, *14*(12), pp.7205 (2022). https://doi.org/10.3390/su14127205

14. Verma, D., Nema, S., Agrawal, R., et al., "A different approach for maximum power point tracking (MPPT) using impedance matching through non-isolated DC-DC converters in solar photovoltaic systems", *Electronics*, *11*(7), pp.1053(2022).
https://doi.org/10.3390/electronics11071053

15. Koutroulis, E., Kalaitzakis, K., Voulgaris, N.C. "Development of a microcontroller-based, photovoltaic maximum power point tracking control system", IEEE *Transactions on power electronics*, 16(1), pp. 46-54 (2001). https://doi.org/10.1109/63.903988

16. Jalil, M. F., Khatoon, S., Nasiruddin, I., et al., **"**Review of PV array modelling, configuration and MPPT techniques", International Journal of Modelling and Simulation, pp. 1–18 (2021). https://doi.org/10.1080/02286203.2021.1938810

17. Danandeh, M.A.; Mousavi G., S.M. "Comparative and comprehensive review of maximum power point tracking methods for PV cells", Renewable *and Sustainable Energy Reviews* (2017). https://doi.org/10.1016/j.rser.2017.10.009

18. Femia N, Petrone G, Spagnuolo G, and Vitelli M. "Optimization of perturb and observe maximum power point tracking method", *IEEE Transactions on Power Electronics*, vol. 20, no.4, pp. 963-973 (2015). https://doi.org/10.1109/TPEL.2005.850975

19. Shchur I, and Turkovskyi V. "Comparative study of brushless DC motor drives with different configurations of modular multilevel cascaded converters*", In 2020 IEEE 15th International Conference on Advanced Trends in Radioelectronics, Telecommunications and Computer Engineering* (TCSET), pp. 447-451 (2020).

https://doi.org/10.1109/TCSET49122.2020.235473

20. Mohanraj, D., Aruldavid, R., Verma, R., et al., "A review of BLDC Motor: State of Art, advanced control techniques, and applications", *IEEE Access* (2022). https://doi.org/10.1109/ACCESS.2022.3175011

21. Zhang, M., Cheng, M., & Zhang, B. "Sensorless control of linear flux-switching permanent magnet motor based on improved MRAS", *In 2018 IEEE 9th International Symposium on Sensorless Control for Electrical Drives (SLED)*, pp. 84-89 (2018). https://doi.org/10.1109/SLED.2018.8486093

22. Madichetty, S., Mishra, S., & Basu, M. "New trends in electric motors and selection for electric vehicle propulsion systems", *IET Electrical Systems in Transportation*, *11*(3), pp. 186-199 (2021). https://doi.org/10.1049/els2.12018

23. Bahrami, M., Mokhtari, H. and Dindar, A. **"**Energy regeneration technique for electric vehicles driven by a brushless DC motor", IET *Power Electronics*, 12(13), pp.3397-3402 (2019). https://doi.org/10.1049/iet-pel.2019.0024

List of Figures

List of Tables

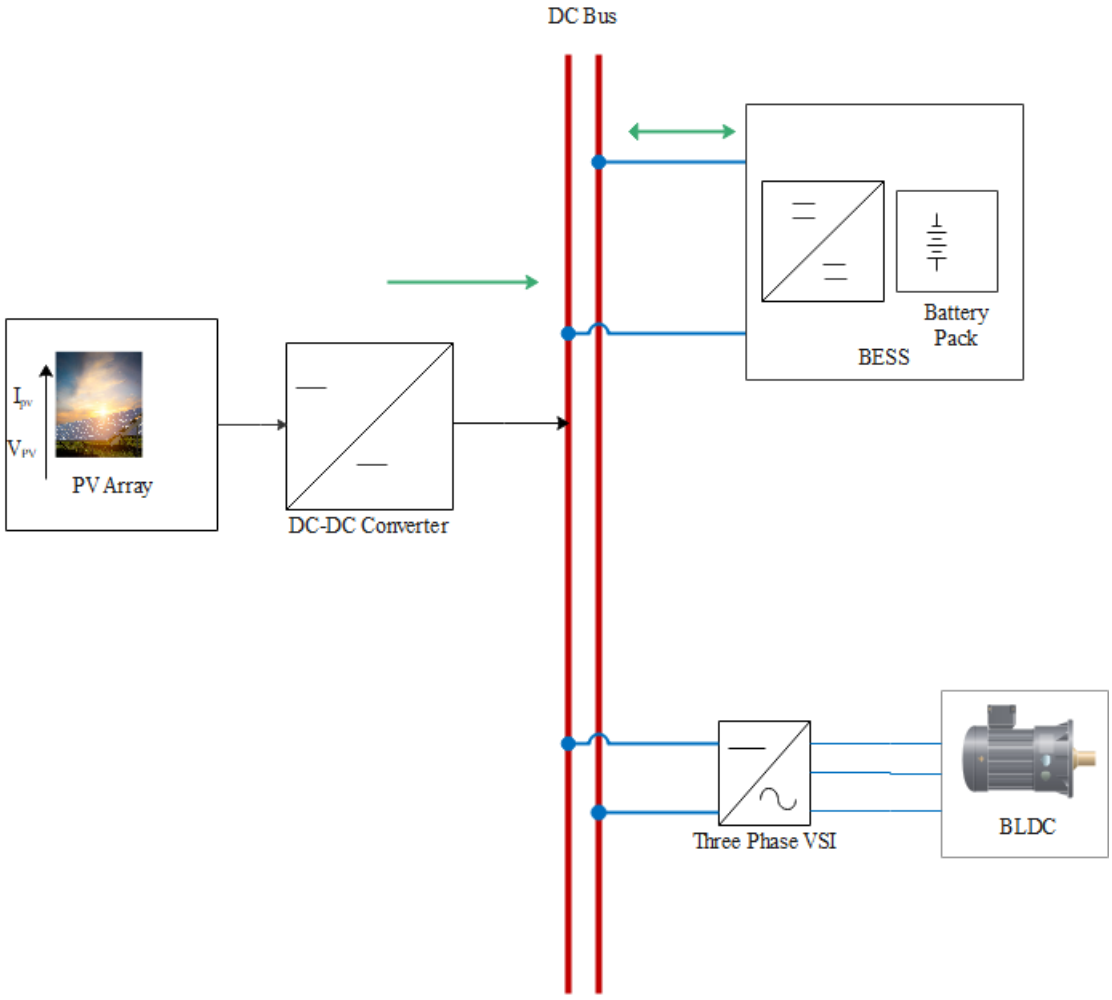

Figure 1. Schematic representation of PV feed BLDC motor drive

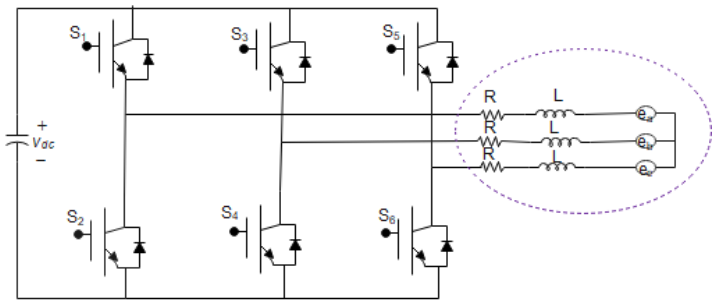

Figure. 2 Circuit representation of BLDC drive

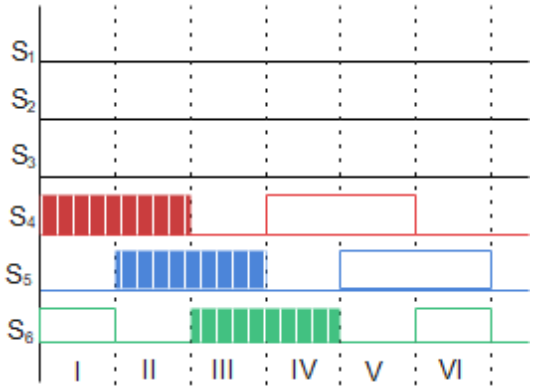

Figure. 3 Switching pulses of VSI during regenerative braking

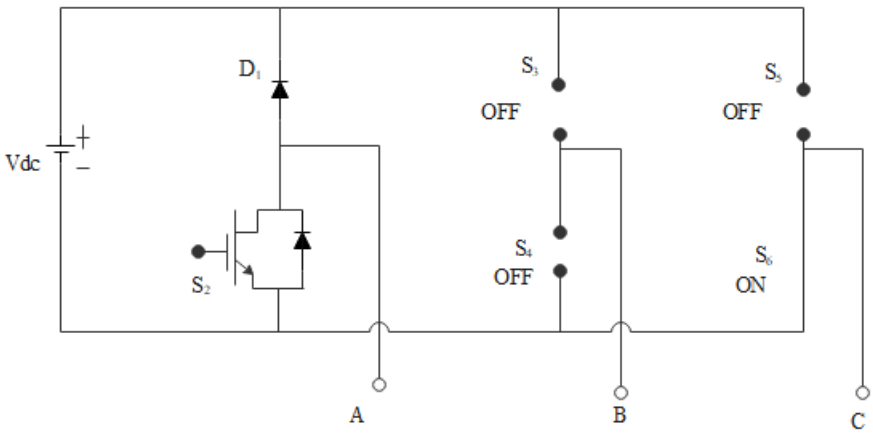

Figure 4(a). Driver circuit of BLDC motor during regenerative braking in single boost method

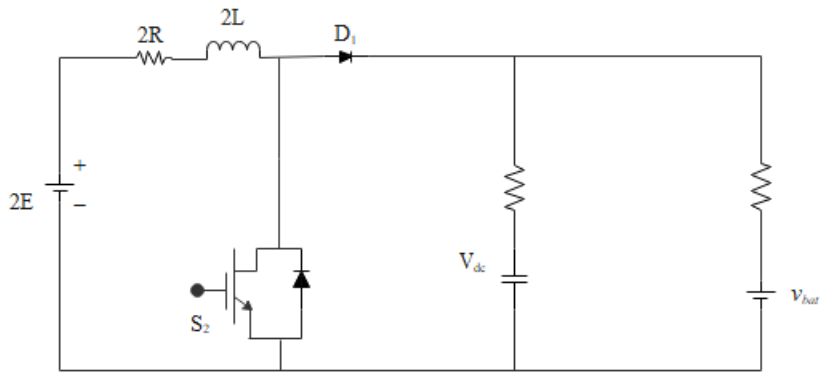

Figure 4(b). Simplified circuit diagram of BLDC driver circuit

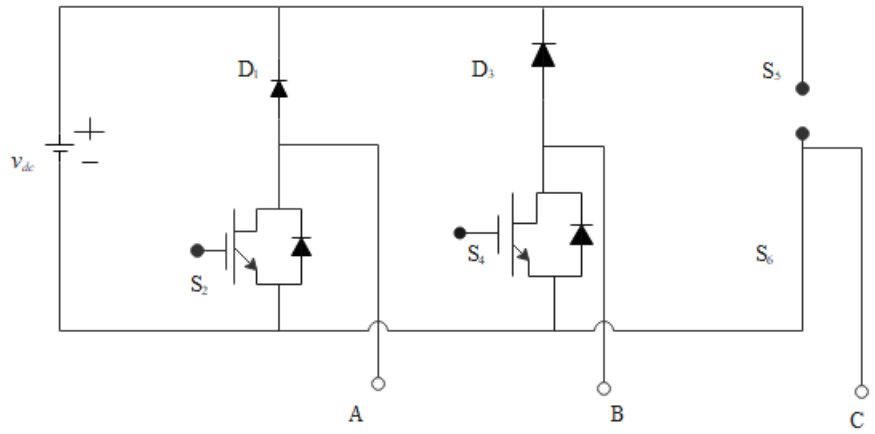

Figure 5. During regenerative braking Driver circuit of BLDC motor in two boost method

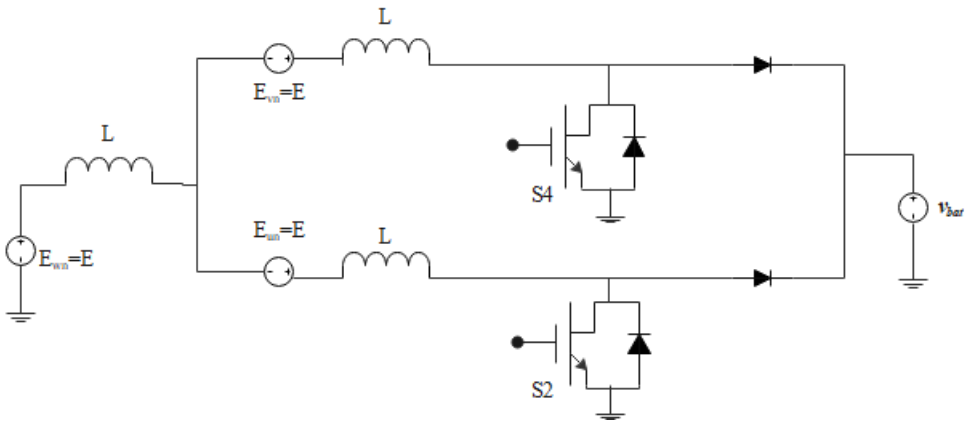

Figure 6. Equivalent circuit diagram of BLDC driver circuit

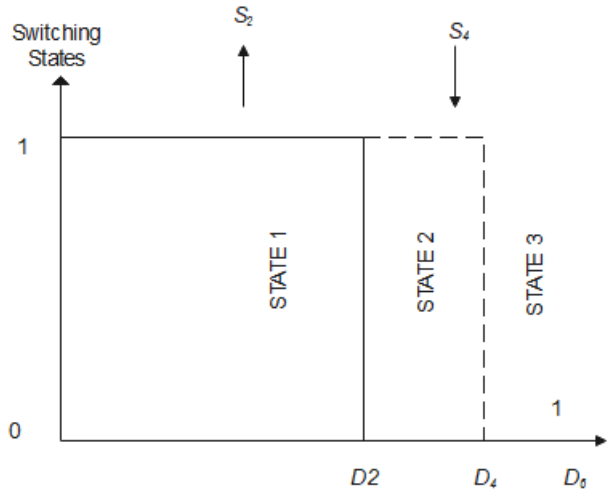

Figure 7. Duty cycle and switching level of the switches

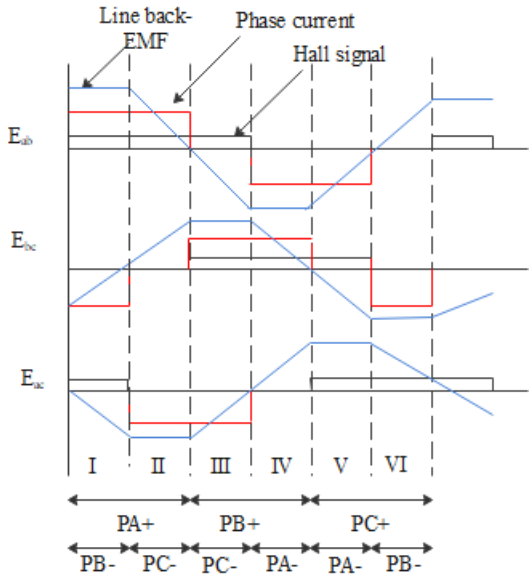

Figure 8. Schematic of Back-emf zero crossing

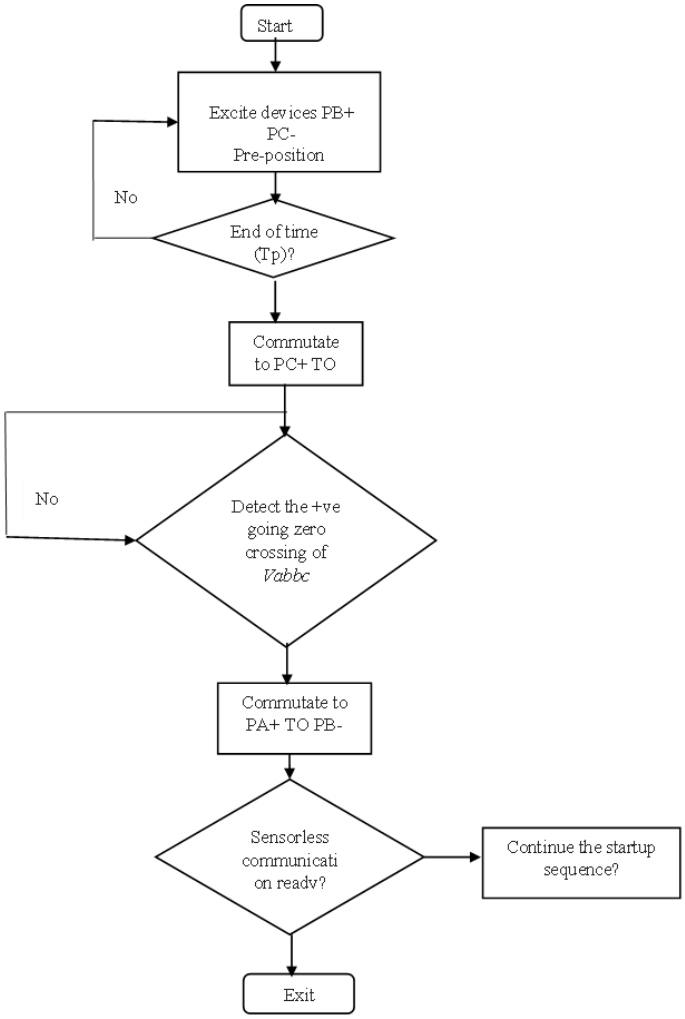

Figure 9. Flow diagram of the control technique

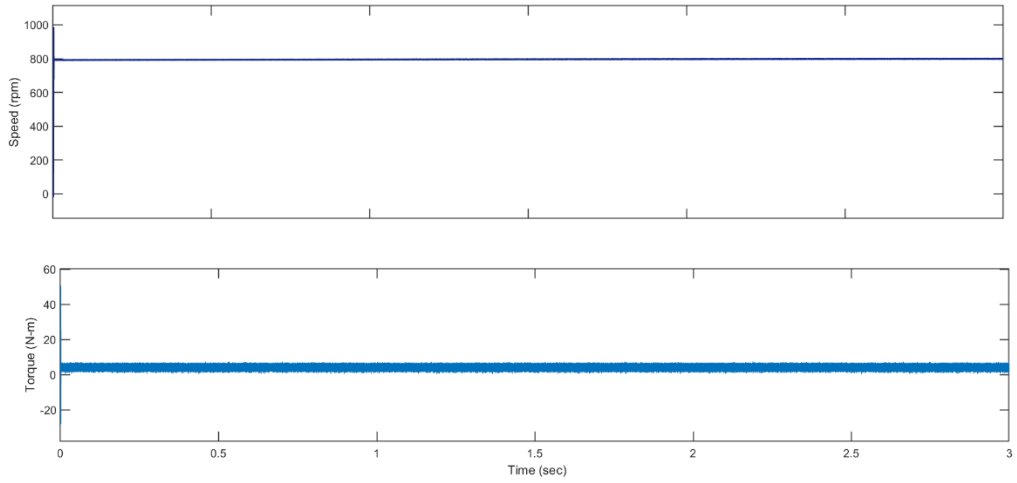

Figure 10. Speed, electromagnetic torque waveform of BLDC motor drive

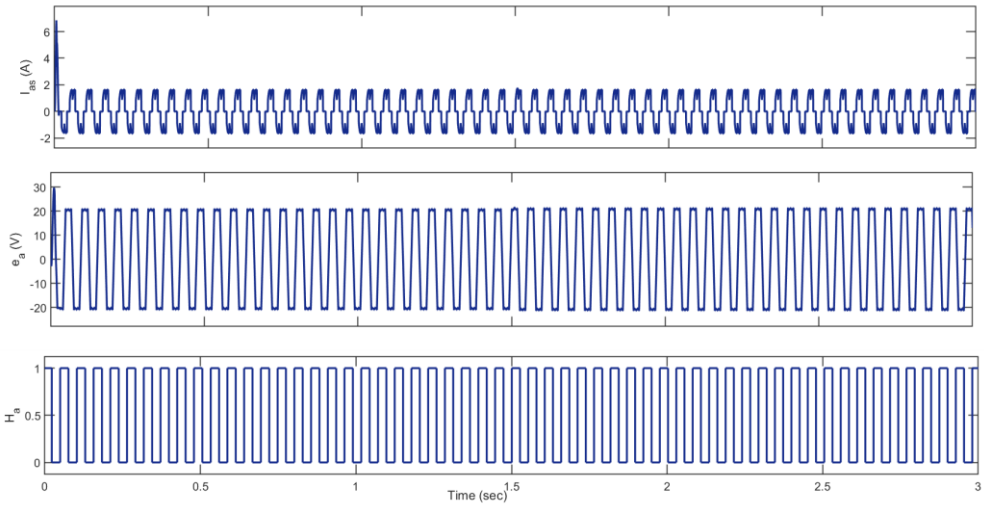

Figure 11. Stator current, electromotive force and Hall Effect of phase A of BLDC Motor

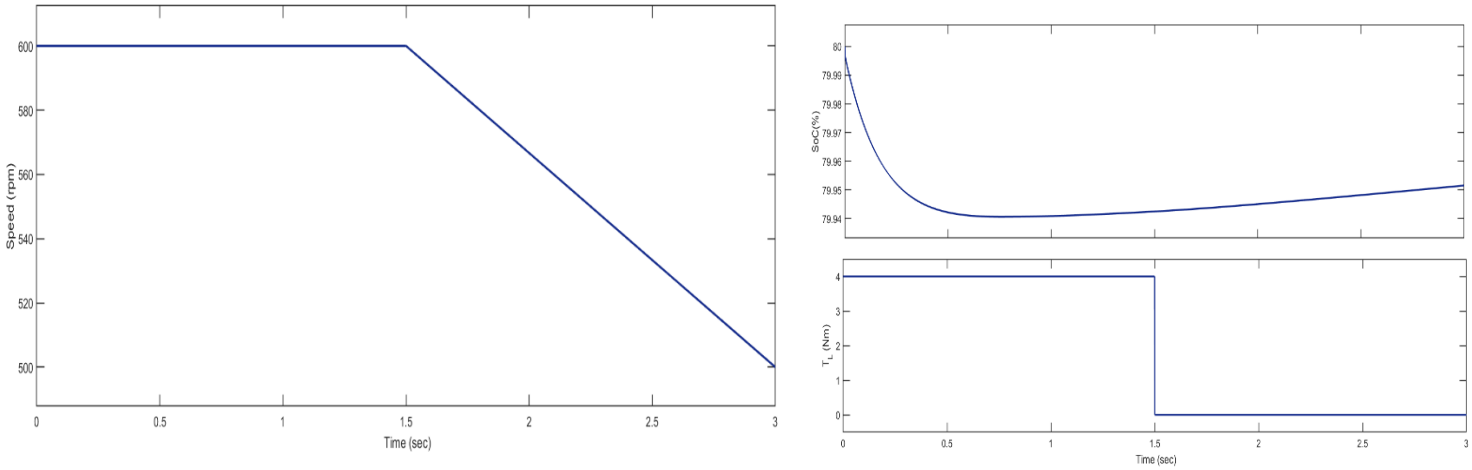

Figure 12. Motor speed, SOC and torque in regeneration mode

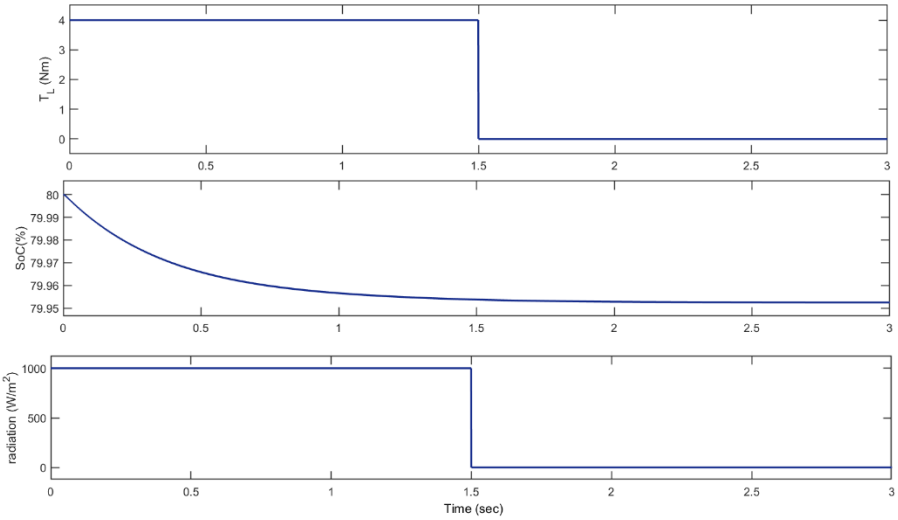

Figure 13. Load torque, battery SoC and solar insolation

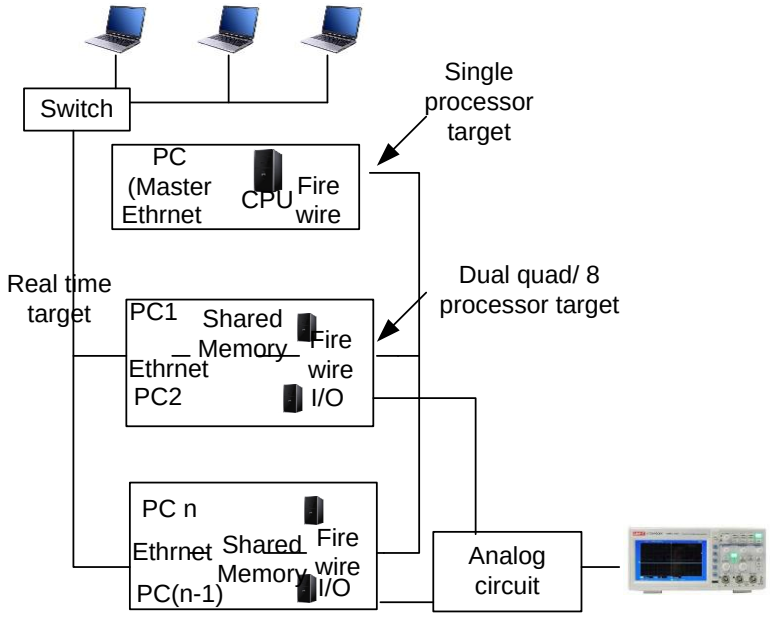

Figure 14. Presentation of RT-Lab simulator architecture

Figure 15. Hardware setup of RT-Lab

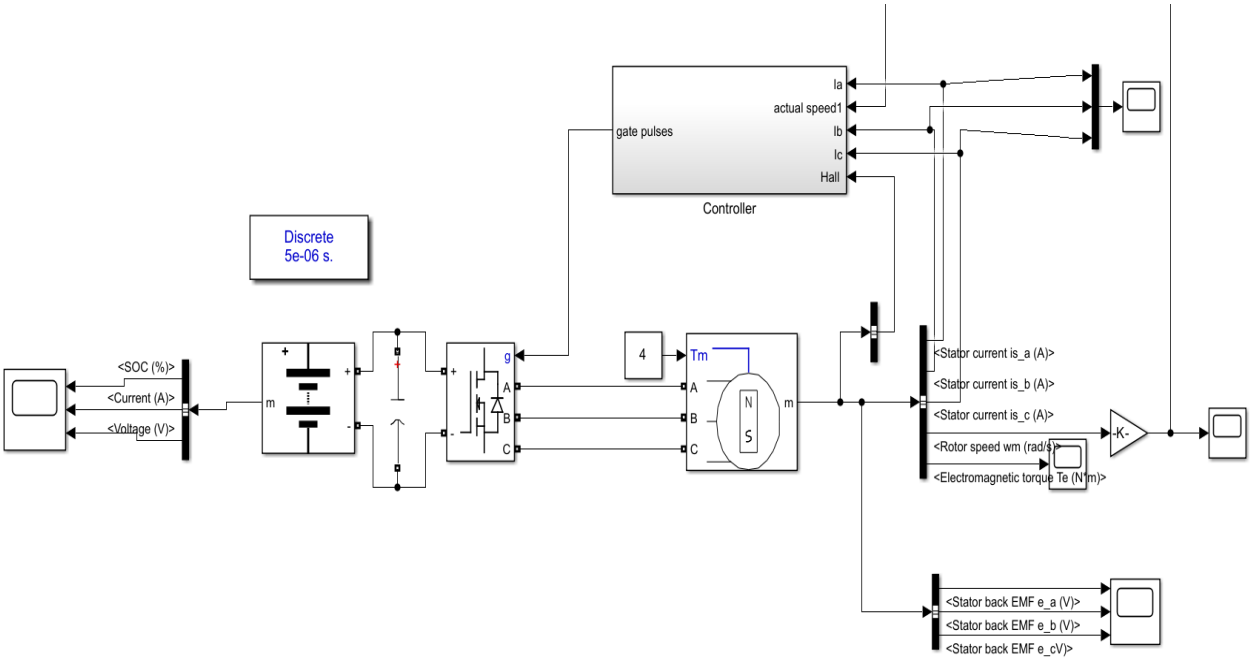

Figure 16. Configuration of the SM_main subsystem

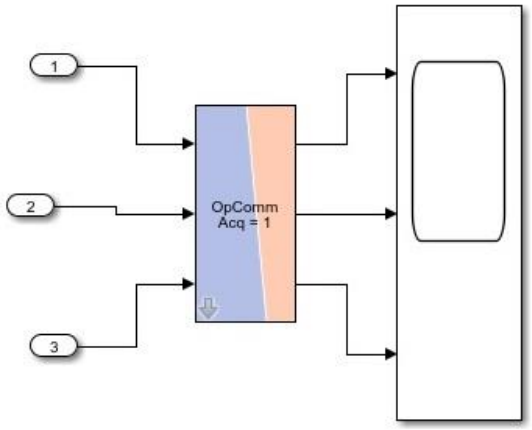

Figure 17. Configuration of the SC_main subsystem

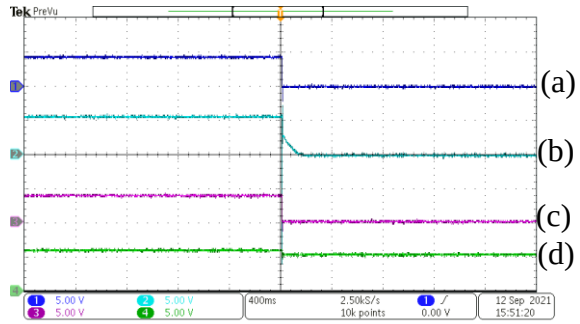

Figure 18. RTDS Hardware results for PV panel (a) P_{PV}(50W/div), (b) V_{PV}(10V/div), (c) I_{PV} (10A/div), (d) V_{out} (10V/div)

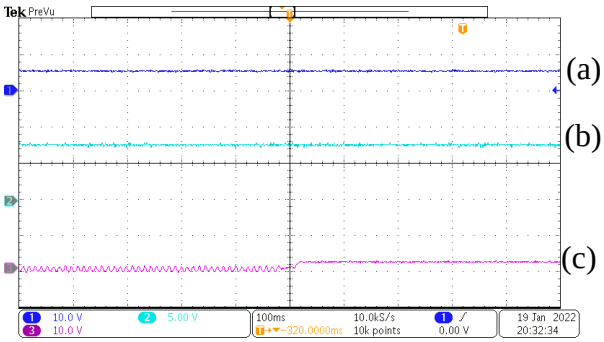

Figure 19. RTDS Hardware results for lithium-ion battery (a) SOC (20/div), (b) V_{bat} (10V/div), (c) I_{bat} (5A/div)

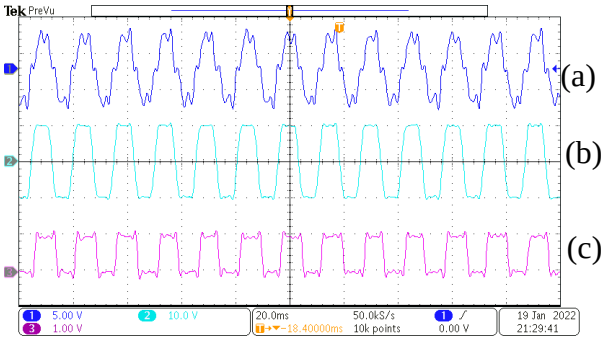

Figure 20. Real time results obtained for BLDC motor drive parameters: (a) I_s(50V/div), (b) e_a (5V/div), (c) H_a(5unit/div)

Table 1. PV array parameter values

Parameters	Values
Power (W_p)	300 W
V_{oc}	45.07 Volts
V_{mp}	25.1Volts
I_{sc}	8.91Amps
I_{mp}	8.54Amps

Table 2. Specification of boost converter

Parameter	Expression	Value
Output voltage	V_o	48 Volts
Input voltage	V_{in}	34 Volts
Duty Cycle	$D = 1 - (V_{in}/V_O)$	0.17-0.85
Inductance	$L = V_{in}\, D/(2\Delta il F_{sw})$	1.75 mH
Output capacitance	$C = I_O D/(\Delta V F_{sw})$	1.8 μF

Table 3. Specification of buck-boost converter

Parameter	Expression	Value
Inductance	$L_b = \frac{V_{bat}\, D}{\Delta I_L F_{sw}}$	1.2 mH
Switching frequency	F_{sw}	5kHz

Table 4. Specification of battery

Parameter	Value
Nominal voltage	48 Volts
Rated Capacity	80 Ah
State-of-charge	80%
Battery response time	1 sec

Table 5. Specification of BLDC motor

Parameter	Value
Stator resistance (R_s)	0.8 ohms
Stator inductance (L_s)	5mH
k_E	1.0V/rad
k_r	70V/krmp
Rated power	1 kW
J	1.12kgm^2
Voltage	48 V
Poles	8

Table 6. Switching sequence

ON switches	Floating phase	Differences of Line voltage	zero crossing	ON-Next switch
PA+ PB-	C	V_{bcca}	positive	PA+ PC-
PA+ PC-	B	V_{babbc}	negative	PB+ PC-
PB+ PC-	A	V_{caab}	positive	PB+ PA-
PB+ PB-	C	V_{bcca}	negative	PC+ PA-
PC+ PA-	A	V_{abbc}	positive	PC+ PB-
PC+ PB-	B	V_{caab}	negative	PA+ PB-

Table 7. Comparative study of proposed drive to commercial drive

Aspects	Commercial Sensor-Based Drive	Sensorless Drive
Startup and Initialization	Offers instant motor startup and precise initialization	May have limitations during startup, resulting in slower acceleration
Performance	Provides superior performance, ideal for applications demanding precise speed and position control	Suitable for applications with relatively stable loads where exact position control is not crucial
Noise and Efficiency	Optimizes motor operation, reduces noise, and improves energy efficiency across a wide range of conditions	Can be noisier and less energy-efficient, especially at low speeds or during transient operation
Environmental Conditions	Better equipped to handle dynamic environmental conditions and load changes	Better for applications with relatively stable environments and load conditions
Reliability	Highly reliable, offering precise control, even in dynamic conditions	Less reliable in applications with high load variations or rapid speed changes
Cost	Higher cost due to the need for position sensors	Cost effective due to absence of sensor.

Table 8. Different protection schemes of BLDC motor

Concern	Protection mechanism	Implementation
Overcurrent protection	Current limiting	Limits current during abnormal conditions (short circuits, load changes).
	Inrush Current Protection	Limits current during startup to prevent excessive inrush currents.
EMC (Electromagnetic compatibility)	EMC Filters	Filters on input and output sides to suppress high-

		frequency noise.
EMI (Electromagnetic interference)	Motor Cable Design	Utilizes shielded cables with proper grounding to minimize electromagnetic interference.
Voltage and Surge Protection	Surge Protection Devices (SPDs)	Diverts excess voltage away from the drive during surges or transients.

Table 9. Performance parameters of different methods

Regeneration Method	**K.E. (Ws)**	**Ereg (W)**	**Ewaste (W)**	η_{reg}
Single boost (open-loop) [23]	505	35	470	6.9%
Two-boost (open loop) [23]	505	80	425	15.8%
Two-boost (closed loop)	1644.39	80	320	19.45%

Biographies

Arpita Basu received the M.Tech degree in Power System from the WBUT, India, in 2013. She is currently pursuing Ph.D. degree in the Department of Electrical Engineering, NIT Jamshedpur, Jharkhand, India. Her research interests include renewable energy resources, electric vehicle, converters.

Madhu Singh graduated in Electrical Engineering from NIT, Patna in the year 1990, post-graduated from NIT, Jamshedpur, in Power Electronics and Drives in 2007. She has completed her Ph.D. in power electronics from NIT Rourkela in 2014. At present she is working as Associate Professor in the Department of Electrical and Engineering in NIT Jamshedpur, India. She has authored many research papers in the areas of Power Electronics and Drives, Renewable Energy Source, Fuzzy Logic Controller and Nonlinear controllers.

Mrs. Singh is a member of IEEE , fellow of IETE. She has supervised 5 Ph.D research scholars.